

# Collisionless Damping of Fast MHD Waves in Magneto-rotational Winds

T. K. Suzuki<sup>1</sup>, H. Yan<sup>2</sup>, A. Lazarian<sup>2</sup>, & J. P. Cassinelli<sup>2</sup>

stakeru@scphys.kyoto-u.ac.jp

yan, lazarian, cassinelli@astro.wisc.edu

## ABSTRACT

We propose collisionless damping of fast MHD waves as an important mechanism for the heating and acceleration of winds from rotating stars. Stellar rotation causes magnetic field lines anchored at the surface to form a spiral pattern and magneto-rotational winds can be driven. If the structure is a magnetically dominated, fast MHD waves generated at the surface can propagate almost radially outward and cross the field lines. The propagating waves undergo collisionless damping owing to interactions with particles surfing on magnetic mirrors that are formed by the waves themselves. The energy damping rate is especially effective where the angle between the wave propagation and the field lines becomes moderately large ( $\sim 20$  to  $80^\circ$ ). The angle tends naturally to increase into this range because the field in magneto-rotational winds develops an increasingly large azimuthal component. The dissipation of the wave energy produces heating and acceleration of the outflow. We show using specified wind structures that this damping process can be important in both solar-type stars and massive stars that have moderately large rotation rates. This mechanism can play a role in coronae of young solar-type stars which are rapidly rotating and show X-ray luminosities much larger than the sun. The mechanism could also be important for producing the extended X-ray emitting regions inferred to exist in massive stars of spectral type middle B and later.

*Subject headings:* magnetic fields – plasma – magnetohydrodynamics – stars : winds – waves

## 1. Introduction

A wide range of stellar classes are thought to have hot plasmas with temperatures greater than  $10^6$  K in their atmosphere. Main sequence stars with low to intermediate mass, including the sun, are known to possess hot coronae, and stellar winds emanate from coronae by thermal expansion most likely enhanced by magnetic wave energy deposition. Magnetic fields generated by dynamo mechanisms in these stars are likely brought to the surface by magnetic buoyancy in the convection zones (Parker 1966), and the fields play a major role in the structure of the outer atmosphere. In a static atmosphere, the gas pressure,  $p$ , falls exponentially with a scale height  $H$ , but the magnetic field,  $B$ , generally decreases more slowly, as a power-

law with radius  $r$ , to satisfy conservation of magnetic flux. As a result, the magnetic pressure,  $B^2/8\pi$ , can eventually dominate thermal pressure from a certain radius outward, even though the thermal pressure dominates in regions nearer the photosphere. Thus in the outer regions the dissipation of the magnetic energy can greatly influence the energetics and dynamics of the atmosphere and wind, producing in some way, the heating of coronae and the wave acceleration of stellar winds. We intend to explore a wave damping process that can produce the heating and acceleration.

Stellar rotation is also closely related to the coronal activities. The observed X-ray luminosity of low to intermediate mass stars increases monotonically with decreasing rotation period,  $P$  for  $P \gtrsim$  several days, and then is saturated for smaller values of  $P$  (Pizzolato et al. 2003). It is likely that the stronger differential rotation in the interior leads to the generation of a surface magnetic field that is stronger, and a more active corona is formed. However, even qualitative ar-

<sup>1</sup>Department of Physics, Kyoto University, Kitashirakawa, Kyoto, 606-8502, Japan; JSPS Research Fellow

<sup>2</sup>Department of Astronomy, University of Wisconsin, 475 N. Charter St., Madison, WI 53706

gments are still lacking as to how the heating and acceleration by the wave damping actually occurs in the atmospheres of rotating stars.

It is now becoming more evident that the heating and driving effects of magnetic fields is not confined only to cool stars, but can be important in the more massive early type stars as well. For many years it had been believed that dynamo generated magnetic fields would not exist on hot stars, and that the winds from these objects were produced only as a result of radiation pressure gradients. Unlike the cooler stars, the hot massive stars do not have an outer convection zone, so the mechanism for the rise of magnetic fields and the source of mechanical energy for coronal heating are not present. However, early UV spectra of the stars showed lines from anomalously high ionization stages (Lamers & Morton 1976). This superionization could be explained as resulting from X-ray ionization by the Auger Effect (Cassinelli & Olson 1979). It was soon realized from satellite observations that essentially all O and B stars are X-ray sources (Seward et al. 1979; Berghöfer et al. 1997), but the nature of the source of the X-rays remained a mystery. Cassinelli & Swank (1979) provided arguments that perhaps there are both shocks in the winds (as proposed by Lucy 1982), as well as hot coronal regions at the base of the winds. This idea that there are two contributors to the X-ray emission has persisted (Waldrön and Cassinelli, 2000). Also, in the case of B near main sequence stars, Cohen et al.(1996) found that the X-ray emission measure was comparable-to or larger than that of a theoretically predicted wind, and hence the coronal component of the X-ray emission could be dominant for these stars. As for the magnetic fields in the outer atmospheres and winds, some direct measurements have been made in near main sequence B stars with fields of about 300 Gauss (Donati et al. 2001). Charbonneau and MacGregor (2001) have shown that fields can be generated by a dynamo operating at the interface between the convective core and the radiative envelope in early type stars. MacGregor and Cassinelli (2003) have shown that such fields can buoyantly rise through the radiative zone to the surface of hot stars. In addition there is a wide variety of observational evidence that hot stars have magnetic fields (Henrichs 2002).

Thus, there appears to be a greater similarity between hot and cool stars than had been envisioned, and it is both timely and useful to consider the processes by which magnetic fields can heat and accelerate winds across the HR diagram. Here the focus is on structures

in which the field in the wind is configured in the form of a spiral, as would naturally arise from the rotation of a star with a magnetic field rooted in its surface (fig. 1) (Weber & Davis 1967; Belcher & MacGregor 1976).

Magnetohydrodynamic (MHD) waves are widely regarded as producing mechanisms that play a role in the heating and acceleration of the outer atmospheric plasmas. Surface turbulence and transient activities (e.g. Sturrock 1999) excite MHD waves at the surface of the sun. It is natural to expect that similar excitation phenomena occur on other stars that have surface magnetic fields. Outwardly propagating MHD waves carry Poynting flux energy, and any dissipation of this flux directly leads to conversion from magnetic energy to thermal and kinetic energy in upper atmosphere. There are numerous studies of wave heating in the solar corona / wind (e.g. Belcher 1971) and in stellar coronae / winds (e.g. Hartmann & MacGregor 1980). MHD waves are discussed in regards to pulsar winds as well (Lyubarsky 2003).

A flow of wave-like motions created by turbulence in a localized source can be decomposed into three types of MHD waves: fast, Alfvén , and slow modes (see Cho & Lazarian 2003). In a magnetically dominated plasma, the slow mode essentially corresponds to an acoustic wave, hence, it probably does not contribute the dominant amount of heating to the plasma in the absence of other strong driving mechanisms (as discussed in §5.3). The fast and Alfvén modes, however, can play a dominant role since their wave energies can easily exceed the thermal energy. These two modes propagate quite differently. The Alfvén waves propagate as transverse waves and only along the field lines, while fast waves can propagate almost isotropically. The properties of fast mode wave do depend on the direction of the wave relative to the magnetic field line and thus can change with radial distance from the star. The component of the fast mode wave which is traveling along the field line is transverse, as is the case for the Alfvén mode, but the fast wave becomes increasingly compressive as the angle,  $\theta$ , between the wave propagation vector and the field line increases.

Some of the properties of the wave propagation are affected by the rotation of the star because the rotation causes the magnetic field lines that are rooted on the star to form a spiral pattern as described above. In the solar wind, the field is usually pictured as developing a so-called Parker spiral (Parker 1963). This spiral arises in spite of the relatively slow rotation of the Sun. More tightly wrapped spiral patterns should

form in the winds of stars that rotate faster, such as younger solar-mass stars and massive stars. Thus, it is important and interesting to study outward propagation of the fast MHD waves in magneto-rotational winds of rapidly rotating stars in general.

Let us consider outgoing fast waves emergent from the stellar surface. The fast waves will travel almost radially without being refracted providing that the magnetic energy in the plasma dominates the thermal energy. However, as the wave travels away from the surface, the angle of propagation,  $\theta$ , increases monotonically (fig. 1) and the character of the wave changes accordingly. The way in which the dissipation of the waves is influenced by this variation of  $\theta$  is described in (§2), where we also discuss how the stellar rotation plays a dominant role in controlling the wave dissipation and subsequent heating of the stellar atmosphere (§4).

An important aspect in the discussion of stellar plasmas is that they are generally collisionless except in regions very near the surface. This is the case because the mean free path for a Coulomb collision,

$$l_{\text{mfp}} = 9.38 \times 10^7 \text{ cm} \frac{(T/10^6 \text{ K})^2}{(n/10^8 \text{ cm}^{-3})}, \quad (1)$$

is larger than wave length. Thus it is essential for us to consider collisionless processes in the wave dissipation. The fast mode waves suffer collisionless damping (Ginzburg 1961; Barnes 1966), and it is discussed in the context of the heating of the solar wind plasma by Barnes (1968, 1969). Interestingly, the damping rate sensitively depends on  $\theta$  (§2). To date, however, this damping process has not been applied to magnetically dominated winds from rapidly rotating stars. It is the goal of this paper to investigate the importance of collisionless damping for both the heating and acceleration of stellar coronae in which the field has the configuration of a magneto-rotational wind.

## 2. Damping of Fast MHD Waves

In this section, we summarize the physical process of collisionless damping of the fast MHD waves, and we introduce the damping rate. It is useful to compare the collisionless damping process with the one that has often been considered in the literature (Hollweg 1982; Suzuki 2004); the damping of waves through the formation of a fast shock train by the steepening of the wave fronts. We find circumstances in coronae under

which the collisionless damping can become more important than the shock steepening process.

As discussed in Ginzburg (1961), the nature of collisionless damping of a wave can be considered analogous to the creation of radiation by charged particles in magnetic field. The charged particles can emit electromagnetic waves both by their acceleration (which produces cyclotron radiation) and by the Cherenkov effect. By the inverse of these two processes charged particles can absorb the radiation. Similarly, plasmas can absorb energy from plasma waves by a gyroresonance process or by a process analogous to the Cherenkov effect. It is the latter that is of interest to us here. It leads to a dissipation of the plasma waves by a wave-particle interaction, which results in heating and acceleration of the particles that compose the plasma.

The resonance of a wave with the gyro-resonance frequency of ambient thermal ions causes a damping of those wave modes that have a frequency close to the ion-cyclotron frequency (e.g. Leamon et al. 1998). Thermal particles can also be accelerated by an oscillating parallel electric field, as is the case for Landau damping of a wave. A similar mechanism called transit time damping (TTD) operates if the electric field is replaced by moving magnetic mirrors (Barnes 1966). introduced this idea to explain the heating of the solar wind, and (Yan & Lazarian 2004) applied to studies on cosmic ray scattering. In this paper, we consider the TTD of fast MHD waves in rapidly rotating stars. We can reasonably assume a magnetically dominated medium, commonly called a low  $\beta$  plasma. As usual,  $\beta$  is the ratio of the gas pressure  $p_g = \rho a^2$ , to the magnetic pressure,  $p_b = B^2/8\pi$ ,

$$\beta \equiv \frac{p_g}{p_b} = \frac{8\pi\rho a^2}{B^2}, \quad (2)$$

where  $B$  is the magnetic field strength,  $\rho$  is the ambient gas density, and  $a$  is the isothermal sound speed.

The TTD is caused by interactions between magnetic mirrors associated with the fast waves (Figure 2) and particles that have a parallel velocity,  $v_{\parallel}$ , similar to the pattern speed of the mirrors, that is,

$$v_{\parallel} \simeq \omega/k_{\parallel}. \quad (3)$$

This is the Cherenkov condition, and  $\omega$  and  $k_{\parallel}$  are wave frequency and wave number parallel to magnetic field line. Particles which satisfy this condition surf on the mirrors and thus interact with the waves. The damping rate  $\gamma_d$  of fast waves which propagate with an

angle  $\theta$  ( $\simeq 1$  radian) relative to the field line in a plasma of a given  $\beta$  ( $\ll 1$ ), and for the Maxwell-Boltzmann particle distribution is (Ginzburg 1961)

$$\gamma_d = \frac{\sqrt{\pi\beta}}{4} \omega \frac{\sin^2 \theta}{\cos \theta} \times \left[ \sqrt{\frac{m_e}{m_H}} \exp\left(-\frac{m_e}{m_H \beta \cos^2 \theta}\right) + 5 \exp\left(-\frac{1}{\beta \cos^2 \theta}\right) \right], \quad (4)$$

where  $m_H$  and  $m_e$  are the hydrogen and electron masses, and this expression is strictly true only for linear waves in which the velocity amplitude is smaller than the phase speed. Note that  $\theta$  changes owing to the turbulent fluctuations in actual situations (Lazarian & Vishniac 1999; Yan & Lazarian 2004). However, since we are considering small relative amplitude,  $\delta B/B$ , and are primarily interested in the average properties, we choose here to treat  $\theta$  as the average angle between the underlying magnetic field and the wave propagation direction.

The Upper panel of fig. 3 presents  $\gamma_d$  divided by  $\omega$  as a function of the angle  $\theta$  for two values of  $\beta$ ;  $\beta = 0.1$  and  $0.01$ . This collisionless damping is shown in comparison with the damping rate associated with a shock train that is usually used for such discussions. (see the Appendix for a discussion of the damping of waves by the shocks). The rate of the collisionless damping is independent of wave amplitude,  $\delta B$ , because it is a linear process, while it is larger in plasma which have a  $\beta$  value not too far below unity. This is because the parallel speeds of the surfing particles needs to be comparable to fast mode speed for the resonance to occur. If  $\beta$  is too low (i.e. the sound speed is too low), only an insignificant fraction of the thermal particles will have the large values required for the condition given in eq.(3).

Collisionless damping is also quite sensitive to the angle  $\theta$ . The damping rate increases more rapidly than the steepening angle in the range  $\theta$  up to  $\theta \lesssim 80^\circ$ , but then it suddenly decreases as  $\theta$  comes closer to  $90^\circ$ . This dependence on  $\theta$  can be understood by considering two competing factors. In general, the damping increases with  $\theta$  because a magnetic mirror tends to be formed in a more efficient way, as is illustrated in Figure 2. A small separation of the field lines is an indication that a magnetic mirror is formed. The closest distance between the field lines become smaller for larger  $\theta$  so that the mirrors become more reflective even though the amplitudes of the fast waves are the

same. Thus, more particles are interacting with the wave to cause the dissipation. However, when  $\theta$  approaches to  $90^\circ$ ,  $k_\parallel$  becomes small, and the resonance condition (eq. 3) requires a large  $v_\parallel$ . Hence, most thermal particles will no longer be in resonance with the wave, so the damping rate decreases sharply in the  $\theta$  near  $90^\circ$  regime.<sup>1</sup>

On the other hand, the damping caused by the shocks does depend on  $\delta B$  because it is a nonlinear process, and is almost independent of the plasma  $\beta$  value (see Appendix eq.(A12)). So, we adopt  $\beta = 0.01$  for the two cases of the shock damping. The damping rate by the shock steepening also increases with  $\theta$  as in the collisionless process, because fast waves contain a longitudinal, *i.e.* compressional, component as  $\theta$  increases, and they become more dissipative. However, the variation is more weakly dependent on  $\theta$  than is the case of collisionless damping.

The conditions under which the collisionless process exceeds the shock steepening process is further illustrated in the lower panel of fig. 3 which shows on a  $\theta$  versus  $\beta$  plane for two cases,  $\delta B/B = 0.1$  (cross hatched) and  $\delta B/B = 0.01$  (single hatched). Note that the collisionless process tends to become more important for larger values of  $\theta$ , except when  $\theta$  is near  $90^\circ$  and except also for cases in which the  $\beta$  value is too small. As is shown, a fast wave with amplitude  $\delta B/B = 0.01$  will dissipate predominantly by collisionless damping over a wide range of  $\theta$ . Even for the case in which  $\delta B/B = 0.1$ , the collisionless damping is seen to be more important for  $\beta \simeq 0.1$  in an angular region of  $60^\circ \lesssim \theta < 90^\circ$ . These results show that there are interesting physical conditions under which collisionless damping should, from now on, be taken to be the primary process for wave dissipation.

These results have shown that the collisionless damping can be comparable-to, or more important than, shock steepening for the damping of fast waves. In fact, collisionless damping could dominate even more-so. This is because shock steepening could be smaller than we have assumed, for the following reasons. First, when a sinusoidal wave is excited initially, it takes some time for it to steepen to form the shocks before the shock dissipation process can begin. Whereas the collisionless damping works immediately, even for the case of sinusoidal waves. Second,

<sup>1</sup>The former effect appears in the  $\frac{\sin^2 \theta}{\cos \theta}$  term in eq.(4) which increases with  $\theta$ , while the latter effect appears in the exponential terms in eq.(4) which both  $\rightarrow 0$  as  $\theta \rightarrow 90^\circ$ .

the collisionless effects can themselves modify the shock dissipation. In general astrophysical circumstances, each shock in a shock train is considered collisionless, so the plasma is not thermalized by Coulomb collisions, but rather the plasma is randomized because of fluctuations in the magnetic field. In such situations, particles with energy larger than average can move across the front more or less transparently and the conversion from kinetic energy to heat would be less effective, and hence also the shock dissipation would be less. We conclude from this section that our results indicate that it is important to account for collisionless damping of the fast modes for realistic and interesting astrophysical situations.

### 3. Model for Magneto-rotational Winds

Let us consider the outward propagation of the fast MHD waves for the case of magneto-rotational stellar winds. Figure 1 depicts propagation of the fast MHD waves in the rotational winds seen from the pole. Here we adopt a simple split monopole configuration for the magnetic fields and assume that the magnetic axis coincides with the stellar spin axis. Spiral magnetic fields are formed in the equatorial region by the stellar rotation (Weber & Davis 1967; Belcher & MacGregor 1976). We can also reasonably assume that the ideal MHD condition holds in the stellar atmosphere. These are common assumptions for the equatorial region of a magneto-rotational wind.

The plasma itself cannot move across the field lines. However, the fast MHD waves can propagate almost isotropically in a low  $\beta$  plasma. In particular, they can propagate radially, crossing the field lines as illustrated in the figure. Also shown is the increase in the angle  $\theta$  as the wave travels away from the surface. Where the angle  $\theta$  is large, the fast waves suffer collisionless damping, as we discussed in the previous section as long as the wave length,  $\lambda$ , is short enough to satisfy collisionless condition,

$$\lambda < l_{\text{mfp}}. \quad (5)$$

For example, if we consider a fast mode wave with period of 1s, with a phase speed is 1000 km/s traveling in plasma with a temperature of  $2 \times 10^6$  K, the collisionless condition that must be satisfied for the particle density is  $n \lesssim 10^8 \text{ cm}^{-3}$ . In the case of the sun, this density condition holds even in the inner corona. As a result, the wave dissipation process directly leads to heating and acceleration of wind plasma and may have an effect on the wind structure.

In this section, we present a model to explore the collisionless damping of the fast mode for the case of magneto-rotational winds. As we are just beginning to develop an understanding of the basic collisionless damping process, it is too soon to be aiming for a complete and self consistent picture. For example, there are other processes such as shock dissipation argued in the previous section that may still be important. We choose to estimate the energy and momentum that is transferred by the fast wave dissipation in the case of a pre-specified background wind. Then we can discuss the likely influence on the wind energetics and dynamics.

#### 3.1. Approximated Wind Structure

Here we describe a practical method for constructing approximate wind structures in the equatorial plane of the magneto-rotational winds, as discussed in Lamers and Cassinelli (1999). We assume that the wind is isothermal at a temperature  $T$ , and we assume that all the physical quantities depend spatially only on the radial distance,  $r$  in the equatorial plane. For the split monopole magnetic field, the conservation of magnetic flux,  $\nabla \cdot \mathbf{B} = 0$ , fixes radial component of the magnetic field,

$$B_r = \left( \frac{R_\star}{r} \right)^2 B_{r,0}, \quad (6)$$

where  $R_\star$  is stellar radius and  $B_{r,0}$  is radial field strength at the surface where  $r = R_\star$ . It is empirically known that radial velocity distribution of stellar winds can be represented by the “beta velocity law” (here we use the power  $\eta$  to avoid confusion with the plasma  $\beta$  ratio that we have used throughout), thus

$$v_r = v_\infty \left( 1 - \frac{R_\star}{r} \right)^\eta, \quad (7)$$

where  $\eta \simeq 0.5\text{--}3$ . If the rotation is slow, terminal velocity,  $v_\infty$ , is of order the escape velocity,  $v_{\text{esc},0} \simeq \sqrt{\frac{2GM_\star}{R_\star}}$ , where  $M_\star$  is stellar mass.

In rapid rotating stars,  $v_{\text{esc},0}$  may not a good indicator of the terminal velocity, as  $v_\infty > v_{\text{esc},0}$  because the wind is significantly affected by acceleration from the magneto-rotational forces. For these cases, Lamers and Cassinelli (1999) show that  $v_\infty$  is better estimated by the Michel velocity (Michel 1969), which is defined as

$$v_M = \left( \frac{r^4 B_r^2 \Omega^2}{\dot{M}_E} \right)^{1/3} = \left( \frac{R_\star^4 B_{r,0}^2 \Omega^2}{\dot{M}_E} \right)^{1/3}, \quad (8)$$

where  $\Omega$  is angular speed of stellar rotation and  $\dot{M}_E$  is equatorial mass flux rate multiplied by  $4\pi r^2$  and we use,

$$\dot{M}_E = 4\pi\rho v_r r^2 (= \text{const.}) \quad (9)$$

In this paper we adopt

$$v_\infty = \max(v_{\text{esc},0}, v_M). \quad (10)$$

It should be noted that  $v_\infty$  can be estimated by the surface values since both  $v_{\text{esc},0}$  and  $v_M$  are determined at  $r = R_*$ . From here on, we follow convention and call cases with  $v_{\text{esc},0} > v_M$ ,  $v_{\text{esc},0} \simeq v_M$ , and  $v_{\text{esc},0} < v_M$ , the “slow”, “moderate”, and “fast” magneto-rotators, respectively.

We can determine azimuthal field component,  $B_\phi$ , for given  $\Omega$  by the induction equation as

$$\frac{B_\phi}{B_r} = \frac{v_\phi - r\Omega}{v_r}. \quad (11)$$

Azimuthal velocity,  $v_\phi$ , is derived from conservation of angular momentum as

$$v_\phi = r\Omega \frac{\frac{v^2 \mathcal{L}}{r^2 \Omega} - v_{A,r}^2}{v_r^2 - v_{A,r}^2} = r\Omega \frac{\frac{r_A^2}{r^2} v_r^2 - v_{A,r}^2}{v_r^2 - v_{A,r}^2}, \quad (12)$$

where  $\mathcal{L}$  is specific angular momentum,  $v_{A,r} = \frac{B_r}{\sqrt{4\pi\rho}}$  is radial Alfvén speed, and  $r_A$  is Alfvén point at which  $v_r = v_{A,r}$ . Thus, we have set the structures of the magneto-rotational winds for given  $M_*$ ,  $R_*$ ,  $\dot{M}_E$ ,  $B_{r,0}$  and  $S_0$ , where  $S_0$  is spin normalized by Kepler velocity,  $\Omega_K = \sqrt{\frac{GM_*}{R_*^3}}$ :

$$S_0 \equiv \frac{\Omega}{\Omega_K} \quad (13)$$

### 3.2. Wave Propagation

We introduce formulation describing propagation of the fast MHD waves with dissipation in the magneto-rotational winds under the WKB approximation. We only consider magnetically dominated *i.e.*, low  $\beta$  plasmas. Accurately speaking, refraction affects the wave propagation; the fast wave propagates toward a region with smaller phase speed,  $v_f$ , defined as<sup>2</sup>

$$v_f = \frac{B}{\sqrt{8\pi\rho}} \left[ 1 + \frac{4\pi\rho a^2}{B^2} \right]$$

<sup>2</sup>Although adiabatic sound speed should appear here, we use isothermal sound speed,  $a$ , as we assume the isothermal atmosphere.

$$+ \sqrt{\left( 1 + \frac{4\pi\rho a^2}{B^2} \right)^2 - \frac{4B_r^2}{B^2} \frac{4\pi\rho a^2}{B^2}} \right]^{1/2}, \quad (14)$$

which corresponds to a direction away from the field line, and where  $B = \sqrt{B_r^2 + B_\phi^2}$ . However, in the case of a low  $\beta$  plasma we can reasonably assume that the fast waves propagate radially without suffering the refraction, because  $v_f \simeq \frac{B}{\sqrt{4\pi\rho}}$  is almost independent of  $\theta$ .

The energy flux of MHD waves in fluids moving with velocity,  $v$  is written as (Jacques 1977)

$$\mathbf{F}_w = \mathbf{V}_g \mathcal{E}_w + \mathbf{v} \cdot \mathbf{p}_w \quad (15)$$

where  $\mathcal{E}_w$  is wave energy density,  $\mathbf{V}_g$  is group velocity, and  $\mathbf{p}_w$  is wave pressure. For a wave amplitude,  $\delta v$ , the energy density is  $\mathcal{E}_w = \frac{1}{2}\rho\delta v^2$ . The energy flux,  $\mathbf{F}_w$ , changes according to work done by  $\mathbf{p}_w$  and damping energy loss rate,  $-Q_w$ , so that in steady state,

$$\nabla \cdot \mathbf{F}_w - \mathbf{v} \cdot (\nabla p_w) = -Q_w. \quad (16)$$

Note that  $Q_w$  works as a heating term for the surrounding plasma. We are focusing on fast MHD waves in the low  $\beta$  plasma. Thus the radial components of the pressure gradient,  $\nabla p_{fw}$ , and the energy flux,  $\mathbf{F}_{fw}$ , can be expressed as (Jacques 1977)

$$(\nabla \cdot \mathbf{p}_{fw})_r = \left( \frac{1}{2} + \sin^2 \theta \right) \frac{d\mathcal{E}_{fw}}{dr} + \frac{3\mathcal{E}_{fw}}{r} \sin^2 \theta \quad (17)$$

and

$$F_{fw,r} = \mathcal{E}_{fw} \left[ \left( \frac{3}{2} + \sin^2 \theta \right) v_r + v_f \right]. \quad (18)$$

The term  $\gamma_d$  in eq. (4) is defined as the damping rate with respect to normalized amplitude,  $\delta w \equiv \delta v/v_f$ . Substitutions of eqs.(17) and (18) into eq. (16) gives an expression for the variation  $\delta w$  in the stellar winds.

$$\begin{aligned} \frac{d}{dr}(\delta w) = -\delta w & \left[ \frac{\gamma_d}{v_r + v_f} + \frac{1}{2\rho} \frac{dp}{dr} + \frac{1}{v_f} \frac{dv_f}{dr} \right. \\ & + \frac{1}{2(v_r + v_f)} \left\{ \frac{(3 - \sin^2 \theta)v_r + 2v_f}{r} \right. \\ & \left. \left. + \frac{d}{dr} \left\{ \left( \frac{3}{2} + \sin^2 \theta \right) v_r + v_f \right\} \right\} \right], \end{aligned} \quad (19)$$

The first term on the right hand side denotes the collisionless damping. The second term indicates the amplification that occurs in a stratified atmosphere in

which the density  $\rho$  is decreasing. The third term appears because  $v_f$  is used for the normalization of  $\delta w$ . The fourth term is due to geometrical expansion of flow tubes and the variation of  $v_f$

For a given wave frequency,  $\omega$ , the damping rate  $\gamma_d$  ( $= \gamma_d(\beta, \theta, \omega)$ ) is determined by the plasma  $\beta$  (from eq. 2) and the angle  $\theta$  between the propagation direction and the field line, for the assumed radial propagation, that is defined by

$$\theta = \tan^{-1} \left( \frac{B_\phi}{B_r} \right). \quad (20)$$

Thus we see that the damping rate,  $\gamma_d$ , is fully determined by the background wind properties.

The initial conditions of the outgoing fast mode waves, at the surface of the star, provide the amplitude,  $\delta w_0 \equiv \delta w_0/v_{f,0}$ , and the period,  $\tau (= 2\pi/\omega)$ . In the following calculations, we consider the results for the specific initial amplitude  $\delta w_0 = 0.1$ . In a region close to the surface, the plasma is generally collisional, i.e.  $\lambda (= v_f \tau) < l_{\text{mfp}}$ . In this region, eq. (19), for collisionless damping, is not applicable, so we assume  $\gamma_d = 0$  when solving eq. (19). However, even without the damping,  $\delta w$  decreases because of the rapid increase of  $v_f$ , (see §4). As a result, all other damping processes should not be effective either, so our treatment has acceptably isolated the collisionless damping case. Once the collisionless condition, eq. (5), is satisfied at  $r = r_{\text{cl}}$  and beyond, we can start the outward integration of eq. (19) to determine  $\delta w$ . Using this, we can estimate heating,  $Q_w$ , and find the acceleration,  $-\frac{dp_w}{dr}$ , that is caused by the dissipation of the fast MHD waves.

## 4. Results

For our model of collisionless dissipation of fast MHD waves in a magneto-rotational wind, there are two important requirements. First, a sufficiently large rotation rate is required to create a sufficiently large  $\theta$  for the wave dissipation to occur. Second, stellar winds with moderately low plasma  $\beta$  values, (i.e.  $\beta \sim 0.01 - 0.1$ ) are favored, because the fast waves, which are essentially magnetic waves, can be dominant only for low  $\beta$  plasmas, although the dissipation is suppressed if the  $\beta$  value is too small. (eq. 4).

### 4.1. Solar-type Stars

Moderately low  $\beta$  winds are found in the coronal winds of low to intermediate mass stars. Although the

Sun is certainly one of the candidates in the sense that it is a moderate to late type star, it has a rotation rate that is too slow to produce the large  $\theta$  assumed in our discussion. Observations of F-K (mid- to late-type) stars in open clusters (Barnes 2003) show that stars with age  $\lesssim 100$  Myr have as large spin <sup>3</sup> as  $S_0 \simeq 0.5$ . Thus these are good classes of stars for us to be considering here.

Figure 4 presents result of moderate magneto-rotational wind for  $S_0 = 0.15$  in a solar-mass star ( $M = 1M_\odot$  and  $R = 1R_\odot$ ). We adopt  $B_{r,0} = 8G$  and  $T = 2 \times 10^6 K$  as typical values. A larger mass loss rate,  $\dot{M}_E = 2 \times 10^{-13} M_\odot \text{yr}^{-1}$ , is employed than the present solar value,  $\dot{M} \simeq 2 \times 10^{-14} M_\odot \text{yr}^{-1}$ , because young solar-mass stars are found to have larger mass loss rate (Wood et al. 2002, 2005) possibly as a result of their enhanced coronal activities or stellar rotation.

On the left of fig 4, we show the wind structures as a function of  $r$ . The top panel shows the velocity distributions,  $v_r$  and  $v_\phi$  of our chosen empirical model, and compares them with both  $v_f$  and the rigid rotation speed  $r\Omega$ . The Michel velocity is  $v_M = 1018 \text{ km/s}$ , is selected as  $v_\infty$  following eq. (10). This value is larger than the escape speed,  $v_{\text{esc},0} = 617 \text{ km/s}$ . For the radial velocity distribution, we adopt the velocity law index  $\eta = 3$  (in eq:7), although we find that  $\eta$  only weakly affects the results. It is the difference between  $v_\phi$  and the solid body rotation,  $r\Omega$ , leads to the spiral pattern. The middle panel shows that the angle  $\theta$  increases monotonically up to  $\gtrsim 70^\circ$ . The bottom panel presents the plasma  $\beta$  value (eq. (2)), and it shows that moderately low- $\beta$  circumstances are in fact realized for these calculations.

Once we have chosen the empirical wind structure for a star, we can solve for the propagation of the fast waves by using eq. (19). On the right side of fig. 4, results for wave periods  $\tau = 1, 10, 100 \text{ s}$ . The top panel exhibits variation of  $\delta w$  (solid) in comparison with the no-dissipation case (dashed). Although  $\delta w$  decreases initially owing to the rapid increase of  $v_f$  to satisfy the wave energy equation (16), farther out it is amplified because of the outward propagation through a decreasing density region. Waves with shorter periods,  $\tau$ , suffer greater damping per unit length, so that they dissipate nearer the star.

The middle-left panel of fig.4 shows a role of the wave dissipation on the wind energetics. An equation describing variation of internal energy per unit mass,

<sup>3</sup> $S_0 = 0.005$  for the sun.

$e$ , is written as

$$v_r \frac{de}{dr} + \frac{a^2}{r^2} \frac{d}{dr} (r^2 v_r) - Q_w = 0, \quad (21)$$

where the second term denotes the adiabatic loss rate and the third term is the heating caused by the wave dissipation. In our current study we evaluate the second and third terms using the chosen empirical wind model. We can then determine the magnitude of the heating term for different  $\tau$  (solid) and compare these with the adiabatic cooling rate (dashed). The panel illustrates that the region heated by the waves depends on the value of  $\tau$ . Waves with the smaller values of  $\tau$  heat the inner regions. Note that the heating exceeds the adiabatic cooling in the respective regions, and this indicates that the assumed temperature ( $= 2 \times 10^6$  K) could indeed be maintained by the wave dissipation. In the case of actual stars, the heating could be distributed more uniformly than shown in the figure, if we were to take into account a spectrum of waves and include thermal conduction as well, as will be discussed in (§5.1).

The lower-left panel of fig. 4 shows the wind dynamics. The equation of momentum density is

$$\frac{d}{dr} \left( \frac{v_r^2 + v_\phi^2}{2} \right) + \frac{1}{\rho} \frac{dp_g}{dr} + \frac{1}{\rho} \frac{dp_{fw}}{dr} + \frac{GM_\star}{r^2} - \frac{d}{dr} \left( \frac{r\Omega B_r B_\phi}{4\pi\rho v_r} \right) = 0, \quad (22)$$

(Lamers & Cassinelli 1999), and the second and third terms are accelerations by the gas and the wave pressure, respectively. A fifth term accounts for magneto-rotational acceleration and it consists of centrifugal force and acceleration owing to the slinging effect of the rotating magnetic field. We compare these three terms in ratios relative to the gravitational acceleration, i.e.

$$\begin{aligned} \Gamma_g &= \left| \frac{1}{\rho} \frac{dp_g}{dr} / \frac{GM_\star}{r^2} \right|, \\ \Gamma_w &= \left| \frac{1}{\rho} \frac{dp_{fw}}{dr} / \frac{GM_\star}{r^2} \right|, \\ \Gamma_b &= \left| \frac{d}{dr} \left( \frac{r\Omega B_r B_\phi}{4\pi\rho v_r} \right) / \frac{GM_\star}{r^2} \right|, \end{aligned}$$

The magnitude of these terms has been evaluated using the empirical wind model and the results are shown in the panel. Note that the gas pressure and the magneto-rotational force are almost comparable in the outer region,  $r \gtrsim 10R_\star$ . This shows that it is reasonable to

call the wind “a moderate magneto-rotator”. The figure also illustrates that the wave pressure becomes as effective an acceleration term as these other two components for a magneto-rotational wind. This means that the fast wave damping is equally important in the wind dynamics; thus the wave pressure could further accelerate the wind.

Next, we study effects of rotation rate. In fig. 5, we compare cases of slow rotator ( $S_0 = 0.01$ ) and fast rotator ( $S_0 = 0.5$ ). The angle  $\theta$  is greatly different in both cases as illustrated in a left panel. Accordingly, the waves dissipate more close to the star for the fast rotator (a middle panel), and the heating (and acceleration not shown) for the fast rotator occurs in the inner region (a right panel). As a result, the wave energy effectively dissipates in the case of the fast rotator to heat and accelerate the plasma, while for the slow rotator, the contribution is not as large. This indicates that regions heated by the wave dissipation depend on the stellar rotation even when the same waves amplitudes are incident at the base.

As a star evolves, the spin rate  $S_0$  generally decreases. Using this tendency, we can speculate on how stellar evolution affects the wave dissipation. Observationally, it is known that young solar-type stars have both a more rapid rotation and show a stronger X-ray luminosity than is the case for the sun (Pizzolato et al. 2003). This indicates that some processes are operating to heat the coronae in the younger, more rapidly rotating stars, in addition to the “basal” heating processes occurring in the present solar corona. We suggest that the process of collisionless damping of fast MHD waves can play an important role in the enhanced heating of the coronae and winds and the X-ray source regions of young solar-type stars because it is much more effective in the rapidly rotating young stars.

## 4.2. Massive Stars

We have shown that our process possibly works in low mass main sequence stars with moderately fast rotation. In this subsection, we would like to consider cases of massive stars. Traditionally, massive main sequence stars have not been thought to have activities concerning magnetic fields, i.e. coronae and/or flares, because their interiors have an outer radiative zone which impedes the rise of magnetic fields and there was no known dynamo mechanism that would lead to surface fields. Nevertheless, as we have stated

in §1, there has been increasing observational evidence for surface fields on hot stars. Coronal activities have been considered to explain the X-ray properties of mid to late B-type near-main-sequence stars (Cohen, Cassinelli, & MacFarlane 1997). More recently, MacGregor & Cassinelli (2003) have shown that the massive stars can have a surface field as a result of a buoyant rise through the radiative zone of fields generated at core-envelope interface dynamo. Although the coronal like geometry might be rather different from the less massive stars, we consider it interesting and instructive to apply the same basic model to massive stars.

It is known from observations of spectral lines that early type stars are commonly fast rotators. This is because such a star tends to be rotating quickly after its initial collapse and formation, the lifetimes are rather short, and thus the massive stars are able to persist in having rapid rotation. The observed mass-loss rate,  $\dot{M}_{\text{obs}}$ , of these types of stars is known for given  $M_{\star}$  and  $R_{\star}$  (de Jager, Nieuwenhuijzen, & van der Hucht 1988). Generally,  $\dot{M}_{\text{E}} \gtrsim \dot{M}_{\text{obs}}$  in the magnetorotational winds since equatorial mass flux is larger than polar mass flux. Magnetic activities and/or stellar rotation might further enhance intrinsic  $\dot{M}$  as discussed in the previous subsection. To take into account these effects, we consider  $\dot{M}_{\text{E}} \simeq (1-10)\dot{M}_{\text{obs}}$ . Then, we can construct the wind structure for a certain star after fixing  $B_{r,0}$  and  $S_0$  (§3.1). Here, we would like to introduce a characteristic mass-loss density (Cassinelli et al. 2002) defined as

$$\rho_{\text{c}} \equiv \frac{\dot{M}_{\text{E}}}{4\pi R_{\star}^2 v_{\infty}}. \quad (23)$$

We have found that  $\rho_{\text{c}}$  is a good indicator for our process; the damping of the fast waves work similarly in winds with the same  $\rho_{\text{c}}$  but different  $M_{\star}$ ,  $R_{\star}$ , and  $\dot{M}_{\text{E}}$ . This is because the damping is controlled by density in the winds by way of the plasma  $\beta$  value which appears in eq.(4) for the damping rate.

We now examine the roles of the fast waves in the wind energetics and dynamics for three stellar parameters,  $\rho_{\text{c}}$ ,  $B_{r,0}$  and  $S_0$ . Since our process does not work dominantly in the slow rotators because the value of  $\theta$  is too small in the winds, we study cases with  $S_0 = 0.15$  (moderate rotator) and 0.5 (fast rotator). We investigate the wave propagation in main sequence stars with  $M_{\star} = 1-8M_{\odot}$ .  $R_{\star}$  for a given  $M_{\star}$  is determined by a relation for the main sequence stars (Kippenhahn & Weigert 1990). Temperature is assumed to

be  $T = 2 \times 10^6 \text{ K}$ , independent of  $M_{\star}$ . Several cases of  $\dot{M}_{\text{E}}$  for a fixed  $(M_{\star}, R_{\star})$  are calculated within the range of  $\dot{M}_{\text{E}} = (1-10)\dot{M}_{\text{obs}}$ . We consider waves with  $\tau = 1 \text{ s}$  and  $\delta w_0 = 0.1$  and investigate how the wave dissipation affects the energetics and dynamics for different  $B_{r,0}$ .

As for the energetics, we examine whether the heating integrated with respect to a certain region exceeds the adiabatic cooling integrated in the same region, namely, we determine the condition of  $B_{r,0}$  which satisfies

$$\int_{R_{\star}}^{r_{\text{out}}} dr \rho r^2 Q_{\text{w}} \geq \int_{R_{\star}}^{r_{\text{out}}} dr \rho a^2 \frac{d}{dr} (r^2 v_r). \quad (24)$$

We adopt  $r_{\text{out}} = 10R_{\star}$  to focus on the heating in the inner wind region. We also carry out the similar procedure for the dynamics. We compare the acceleration due to the wave pressure integrated in the same region with the acceleration by the other two components:

$$-\int_{R_{\star}}^{r_{\text{out}}} dr v_r r^2 \frac{dP_{\text{w}}}{dr} \geq -\int_{R_{\star}}^{r_{\text{out}}} dr v_r r^2 \frac{dp}{dr} + \int_{R_{\star}}^{r_{\text{out}}} dr \rho v_r r^2 \frac{d}{dr} \left( \frac{r \Omega B_r B_{\phi}}{4\pi \rho v_r} \right) \quad (25)$$

Figure 6 shows the critical values for  $B_{r,0}$  with respect to the energetics (solid; eq. (24)) and dynamics (dashed; eq. (25)) as a function of  $\rho_{\text{c}}$  in the moderate (thick) and fast (thin) rotators. The collisionless damping of the fast modes can dominate the other processes if the field strength exceeds the respective lines. If  $\dot{M}_{\text{obs}}$  is used when deriving  $\rho_{\text{c}}$  instead of  $\dot{M}_{\text{E}}$  in eq. (23),  $\rho_{\text{c}}$  has one-to-one correspondence to  $M_{\star}$  because dependence of  $\dot{M}_{\text{obs}}$  on  $M_{\star}$  is steep (de Jager, Nieuwenhuijzen, & van der Hucht 1988) while those of  $R_{\star}$  and  $v_{\infty}$  are weaker (Kippenhahn & Weigert 1990). At the top of the figure, we give the spectral type of the stars used to determine  $\rho_{\text{c}}$ . Please note that this is based on  $\dot{M}_{\text{obs}}$ . If a star has larger  $\dot{M}_{\text{E}}$  as discussed previously, its  $\rho_{\text{c}}$  becomes larger than the shown spectral type.

Figure 6 shows that the required value for  $B_{r,0}$  is  $\lesssim 100 \text{ G}$  even in mid to late B stars. This is a reasonable range for these types of stars as has been shown by Maheswaran & Cassinelli (1992). Cassinelli et al.(2002) have shown that such fields are sufficient to play a role in the channelling and torquing of the moderately weak winds of B main-sequence at about spectral type B3V and later. The critical  $B_{r,0}$  is a monotonically increasing function of  $\rho_{\text{c}}$  and a relation,

$B_{r,0}^2/\rho_c \sim \text{const.}$  holds. Since we assume the same gas temperature, the relation can be understood that the similar plasma  $\beta$  is required even for different stellar mass. As  $\rho_c$  increases, the collisionless condition breaks down in the inner regions. On the dotted lines the plasma is still collisional at  $r = 2R_*$  for the waves with  $\tau = 1\text{s}$ . From the magnetic fields, of order 100 Gauss or so, that are required, we can conclude that our process can operate effectively in stars with spectral type of about B3V and later with hot outer atmospheres/winds. Interestingly, this spectral type is consistent with the result, obtained by Cohen, Cassinelli, & MacFarlane (1997), that the X-rays from mid- to late- B type stars seem to be arising increasingly from the presence of extensive hot winds and confined coronal zones.

In both cases of  $S_0 = 0.15$  and  $0.5$ , the condition that the damping dominate the dynamics demands a larger  $B_{r,0}$  than is the case for the energetics. This is because the dynamics condition compares the wave acceleration with both thermal and Poynting processes while the energetics condition compares the damping with the thermal processes (i.e. adiabatic cooling) only. In a region between the two conditions, the wind could be heated by the fast waves, but still accelerated dominantly by the magneto-rotational force rather than by the waves. For the moderate rotators, the wave dissipation is slower and a certain fraction of the wave energy remains at the radius  $r_{\text{out}}$ . Therefore, the magnetic field  $B_{r,0}$  that is required for the energetics condition is larger than that for the fast rotators, and this is to increase the initial wave energy. On the other hand, the dynamics condition shows that the fast rotators demand the larger  $B_{r,0}$ , and this is to let the wave acceleration exceed the magneto-rotational acceleration, which is also larger for the fast rotators.

## 5. Discussion

So far we have studied outward propagation of the fast waves based on several assumptions : (i) wave amplitude at the surface ( $\delta w_0 = 0.1$ ) (ii) monochromatic wave spectrum (iii) no refraction (iv) a fixed, pre-specified magneto-rotational wind. First, we discuss these assumptions. Then, we compare the collisionless damping with the steepening damping and with other types of waves as well. Finally we mention another application of our process, to pulsar wind nebulae.

### 5.1. Limitations of Model

(ii) *Wave Generation* : In §4 we have assumed that  $\delta w_0 = 0.1$  at the inner boundary without specifying processes of the wave generation. The inner boundary does not coincide with the photosphere, but the base of the corona, since we assume  $T = 2 \times 10^6$  throughout the atmosphere. The density generally decreases by several orders of magnitude from the photosphere to the corona, and the region between them is called chromosphere and transition region.

We can consider two types of the wave generators. One type of wave generator is associated with the granulations originating from the surface convection zones which exist in the low- to intermediate stars. The other type of generator corresponds to oscillations of closed magnetic loops emerging from the surface. The up-going waves generated by the former process suffer damping in the chromosphere before reaching the corona (see Stein Schwartz 1972 for sound waves). The closed magnetic loop process directly excites the waves at higher altitude in the corona (Sturrock 1999), and thus is more suitable for the present paper. Stars with faster rotation are expected to have stronger activities involving these magnetic loops (Jardine et al. 2002).

Accordingly,  $\delta w_0$  would be larger in these stars than in stars with slower rotation; probably  $\delta w_0 = 0.1$  is realizable in the fast and moderate rotators by the direct excitation in the corona, while it is less likely in the slow rotators due to the lack of the sufficient activities of the loops. In addition to the difference of the dissipation conditions (§4), the difference of the wave generation processes would be important when discussing the stronger X-ray activities in faster rotating stars.

(ii) *Wave Spectrum* : Although we have only considered the monochromatic waves in the model calculations, they are likely to be injected from actual stars with some spectrum of frequencies, and the wave frequency controls the wave damping as we have shown in the previous section. Namely waves with higher frequencies dissipate in the inner region. If some spectrum (e.g. a power-law in  $\omega$ ) were given for the input waves, the stellar atmosphere would be heated more uniformly; with the inner regions is heated by waves with higher frequencies, and outer regions is heated by those with lower frequencies.

(iii) *Wave Refraction* : We have assumed that the fast mode propagates radially without being refracted. In fact,

the refraction is not negligible unless the plasma  $\beta$  is sufficiently small. This is because the anisotropy of  $v_f$  appears in cases in which the sound speed is not sufficiently small relative to the Alfvén speed (eq. (14)). Generally, a wave is refracted toward a region with a smaller phase speed. For a fast mode wave, it is refracted in a direction away from the field line (toward larger  $\theta$ ). This effect causes the fast wave to dissipate more quickly since the damping increases with the angle  $\theta$ . As a result, we should expect the heated region to be shifted slightly inward as compared with the heated region from the radial propagation that we assumed.

(iv) *Fixed Background* : In this paper, we treat the wave propagation within a given empirical wind structure. We think that this approach is acceptable as a first attempt to assess the importance of heating and acceleration produced by wave dissipation. Needless to say, a self-consistent treatment of the wind structure would be required in a more complete modeling of a star. This is because wave dissipation can directly affect both  $v_r$  (via acceleration) and  $T$  (via heating). These two variables affect other quantities associated with the outflow as well. However, we are of the opinion that empirical  $v_r$  that we have assumed gives reasonable wind structure, simply because the velocity distribution is determined mainly by the basic stellar parameters  $M_\star, R_\star, S_0$ . Figure 6 also illustrated that a stronger field was needed to modify the dynamics than is the case for the energetics.

Given the velocity structure, it is the energetics and the resultant temperature that must be considered more carefully. Unlike the wind velocity, the temperature structure is not determined by the basic stellar parameters but rather by the boundary conditions for the wave generation and the subsequent wave heating and radiative cooling and thermal conduction cooling . An important point for our collisionless process is that the damping rate is controlled by temperature through  $\beta$  value (eq. (4)). Once the plasma is heated, i.e.  $\beta$  increased, by the waves, the damping is enhanced. It leads to further heating until most of the wave energy dissipates. This seemingly catastrophic behavior is partially inhibited in reality by the cooling effects of thermal conduction which become more effective if the temperature increases. In more intensive studies, it would be important to examine the more complicated energetics with the other effects are accounted for.

## 5.2. Collisionless Damping vs. Steepening

We would like to compare the two types of the damping discussed earlier, in light of the magneto-rotational wind results. Figure 3 shows that the collisionless process and steepening work in different regimes, namely the former is important for larger  $\theta$  except  $\theta = 90^\circ$  and smaller  $\delta w \lesssim 0.1$  while the latter dominantly works for smaller  $\theta$  and larger  $\delta w > 0.1$ .

In a stellar atmosphere the amplitude,  $\delta v$ , of the up-going wave is inevitably amplified because the density decreasing. Even the normalized amplitude,  $\delta w$ , increases after the slight decrease in the inner region as shown in the top right panel of Figure 4. In the cases of moderate and fast rotators,  $\theta$  is already large when  $\delta w$  becomes large enough for the dissipation. Therefore, the collisionless damping sets in first.  $\delta w$  is kept small by the collisionless damping in the entire region, which is not suitable for the steepening. In the case of slow rotators, the collisionless damping is not so effective even though  $\delta w$  increases to the same level, because  $\theta$  is still small. As a result, the dissipation of waves through shock steepening is expected to be more important in slow rotating stars.

## 5.3. Other Modes

In this paper we have focused on the fast mode waves. In reality, the three MHD modes couple and have a more-or-less turbulent nature. Since the waves and turbulence are mainly excited from the stellar surface, one has to consider the imbalanced cascade of turbulence in such a situation (Cho, Lazarian, & Vishniac 2002). Also, because of the density stratification, the amplitude of the turbulence would not decrease with radius even in the outer region, far from the surface.

The slow wave has not been considered as a dominant heating source in the solar corona, because the slow waves that are generated from the photosphere dissipate too rapidly (Stein & Schwartz 1972). However, it has been shown that strong driving of the slow mode can possibly occur at higher altitude as a result of the dynamical motion of the closed loops (Sturrock 1999) in young solar type-stars that exhibit strong stellar activities (Ayres 2000). In such a situation, super-sonic slow modes can be important (Beresnyak, Lazarian, & Cho 2005). Slow mode waves suffer TTD, similar to that affecting fast mode waves, and thus contribute to the heating. This will be studied in a forthcoming paper. The steepening would be important as

well (Suzuki 2002).

The Alfvén wave is also a candidate for the heating in the low- $\beta$  solar and stellar plasmas. The Alfvén waves dissipate in density-stratified atmosphere by processes such as phase mixing (Heyvaerts & Priest 1983), nonlinear mode conversion (Cho & Lazarian 2002; Cho & Lazarian 2003; Suzuki & Inutsuka 2005), turbulent cascade triggered by reflection (Oughton et al. 2001). High frequency Alfvén waves suffer ion-cyclotron damping (Cranmer, Field, & Kohl 1999) as well. The dissipative nature of the Alfvén waves, which propagate along the field lines in the magneto-rotational winds is less modified for cases in which the wave length is shorter than the curvature scale of the winding field lines. So, Alfvén waves can operate in both slow and fast rotators and also contribute to the basal heating in stellar coronae. The processes directly linking to the stellar rotation as shown in this paper would give additional contributions to lead to stronger coronal activities in rapidly rotating stars.

#### 5.4. Application to Pulsar Winds

So far we have focused on the collisionless damping of the fast MHD waves in normal stars. This mechanism can work in any situation in which the fast waves travel in a low  $\beta$  plasma with curved magnetic fields. A pulsar wind is one of the candidates. A pulsar magneto-sphere is a low  $\beta$  and collisionless plasma, and the MHD approximation is acceptable because the particles can interact with the waves through the magnetic fields.

Lyubarsky (2003) considered dissipation of the fast waves propagating radially in pulsar winds by multiple shocks as a result of the steepening in order to investigate dissipation of the electromagnetic energy. Because the toroidal magnetic field component dominates owing to the rotation of the pulsars, he studied the fast waves traveling perpendicular to the field lines, i.e.  $\theta = 90^\circ$ . For this specific angle, the collisionless damping is not efficient, as shown in §2, so that the steepening would in fact be the more effective process in the wave dissipation. However, if  $\theta$  is not strictly  $= 90^\circ$ , say because of perturbed magnetic fields or other effects, collisionless damping would again become important. Although beyond the scope of the present paper, relativistic effects should be taken into account in a proper study of collisionless damping in pulsar winds.

## 6. Summary

For the case of magneto-rotationally driven winds, we have considered the heating and acceleration of a stellar plasma caused by the collisionless damping of fast MHD waves. Fast mode waves propagate almost radially even in spiral magnetic fields thanks to the isotropic character of the propagation, provided that the  $\beta$  is low. The plasmas are typically collisionless, so the waves undergo collisionless damping. We find that collisionless damping of fast MHD waves is effective when (i) the angle between the wave propagation and the field line is large and (ii) the plasma  $\beta$  is around  $0.01 - 0.1$ . In the magneto-rotational winds, the angle increases as the wave travels away from the surface. This angle change eventually leads to a dissipation of the waves, and causes heating and acceleration of the surrounding medium.

We have found that our collisionless damping is important in moderate and fast magneto-rotators of solar-mass stars, while it is not so effective in slow rotators such as the (present) sun. It cooperates with the “basal” processes which are responsible for the heating of the corona in the slow rotators. We propose that the mechanism of collisionless damping of fast waves can explain the observed strong coronal activities in young (age  $\lesssim 100$ Myr) solar-type stars because of their rapid rotation. The damping also effectively applies in the energetics, and perhaps also to the dynamics, of the atmospheres of moderately massive main sequence stars of which are of spectral types about B3V or later and which have observationally plausible magnetic fields ( $\lesssim 100$ G).

When compared with the shock dissipation by the steepening, the collisionless damping is expected to be more important in moderate and fast rotators with an input wave amplitude,  $\delta w_0 \lesssim 0.1$ . In addition, the process is also argued to be important in general astrophysical low  $\beta$  plasma which has curved magnetic fields, such as pulsar magneto-spheres.

T.K.S. is supported by the JSPS Research Fellowship for Young Scientists, grant 4607, and acknowledge a Grant-in-Aid for the 21st Century COE “Center for Diversity and Universality in Physics” from the Ministry of Education, Culture, Sports, Science, and Technology (MEXT) of Japan. A.L. and H.Y. acknowledge NSF grant ATM-0312282, and A.L. and J.P.C. also acknowledge the support of the Center for Magnetic Self-Organization in Laboratory and Astrophysical Plasmas.

### A. Damping by Steepening

In this appendix, we summarize the damping of fast shock trains which form by the steepening of fast MHD waves. First, we derive entropy generation at the fast shock whose geometry is shown in fig. 7. Physical quantities in the upstream region are indicated by subscript “1” and those in the downstream region by “2”. Components parallel with shock normal are denoted by subscript “ $\parallel$ ” and those perpendicular to it by “ $\perp$ ”. Because of the conservation of magnetic flux,  $\nabla \cdot \mathbf{B} = 0$ , the parallel component of magnetic field,  $B_{\parallel}$ , is constant. The perpendicular field strength is increased from  $B_{\perp}$  to  $B_{\perp} + \delta B_{\perp}$  at the fast shock. The equations for the conservation of mass flux, momentum parallel and perpendicular to shock normal, electric field, and energy are expressed in the frame of an observer co-moving with the shock as (e.g. Priest & Forbes 2000)

$$\rho_1 v_{\parallel,1} = \rho_2 v_{\parallel,2}, \quad (\text{A1})$$

$$p_1 + \rho_1 v_{\parallel,1}^2 = p_2 + \rho_2 v_{\parallel,2}^2 + \frac{2B_{\perp}\delta B_{\perp} + \delta B_{\perp}^2}{8\pi}, \quad (\text{A2})$$

$$\rho_1 v_{\parallel,1} v_{\perp,1} = \rho_2 v_{\parallel,2} v_{\perp,2} - \frac{B_{\parallel}\delta B_{\perp}}{4\pi}, \quad (\text{A3})$$

$$v_{\parallel,1} B_{\perp} - v_{\perp,1} B_{\parallel} = v_{\parallel,2} (B_{\perp} + \delta B_{\perp}) - v_{\perp,2} B_{\parallel} (= 0) \quad (\text{A4})$$

and

$$\begin{aligned} p_1 v_{\parallel,1} + \rho_1 e_1 v_{\parallel,1} + \frac{B_{\perp}^2}{4\pi} v_{\parallel,1} - \frac{B_{\parallel} B_{\perp}}{4\pi} v_{\perp,1} + \frac{1}{2} \rho_1 (v_{\parallel,1}^2 + v_{\perp,1}^2) v_{\parallel,1} \\ = p_2 v_{\parallel,2} + \rho_2 e_2 v_{\parallel,2} + \frac{(B_{\perp} + \delta B_{\perp})^2}{4\pi} v_{\parallel,2} - \frac{B_{\parallel} (B_{\perp} + \delta B_{\perp})}{4\pi} v_{\perp,2} + \frac{1}{2} \rho_2 (v_{\parallel,2}^2 + v_{\perp,2}^2) v_{\parallel,2}. \end{aligned} \quad (\text{A5})$$

Here we define all the quantities in a frame co-moving with the shock front. Then, both left- and right-hand sides of eq.(A4) become 0. By eliminating  $v_{\parallel,1}$ ,  $v_{\parallel,2}$ ,  $v_{\perp,1}$ ,  $v_{\perp,2}$ , and  $p_2$  from eqs.(A1)–(A5), we have a relation between  $\delta B_{\perp}$  and compression ratio,

$$\sigma \equiv \frac{\rho_2}{\rho_1}, \quad (\text{A6})$$

as

$$-\frac{\gamma p_1}{\rho_1} \frac{\sigma - 1}{\sigma} - \frac{\delta B_{\perp}^2}{8\pi\sigma\rho_1} + \{\gamma + 1 - \sigma(\gamma - 1)\} \frac{\delta B_{\perp}}{8\pi\sigma\rho_1} \frac{\{(\sigma - 1)B^2 - B_{\perp}\delta B_{\perp}\}}{\{\delta B_{\perp} - (\sigma - 1)B_{\perp}\}} = 0, \quad (\text{A7})$$

where  $B^2 = B_{\parallel}^2 + B_{\perp}^2$ . The pressure jump is also derived from eq. (A2) :

$$\Delta p \equiv p_2 - p_1 = \frac{2(\sigma - 1)B^2\delta B_{\perp} + (\sigma - 3)B_{\perp}\delta B_{\perp}^2 - \delta B_{\perp}^3}{8\pi\{\delta B_{\perp} - (\sigma - 1)B_{\perp}\}}. \quad (\text{A8})$$

Entropy generation is written as (Mihalas & Mihalas 1984)

$$\frac{\Delta s}{R} = \frac{1}{\gamma - 1} \ln\left(\frac{p_2 \rho_1^{\gamma}}{p_1 \rho_2^{\gamma}}\right) \simeq \frac{1}{\gamma - 1} \left\{ \ln\left(1 + \frac{\Delta p}{p}\right) - \gamma \ln(\sigma) \right\}, \quad (\text{A9})$$

where  $R$  is a gas constant, and we assume that the shock is weak. Then,  $\Delta s$  is derived from a given amplitude,  $\delta B_{\perp}$ , by using eqs.(A7) and (A8).

The steepening of the wave fronts forms the fast shock train. The wave dissipates by these multiple shocks. The heating rate,  $Q_s$  (erg cm $^{-3}$ s $^{-1}$ ), of the fast shock train with angular frequency,  $\omega$ , is given by

$$Q_s = \frac{\Delta s}{R} \rho_1 R T \frac{\omega}{2\pi} = \frac{\Delta s}{R} p_1 \frac{\omega}{2\pi}. \quad (\text{A10})$$

The damping rate is derived from  $Q_s$  and energy density of the wave,  $\frac{\delta B_{\perp}^2}{8\pi}$ , as

$$\gamma_s = \frac{Q_s}{\delta B_{\perp}^2/8\pi} \quad (\text{A11})$$

Note that if  $\delta B_\perp/B$  is fixed for the weak shocks,  $\gamma_s$  is independent of plasma  $\beta$  because

$$\gamma_s \propto \frac{\Delta s}{R} p_1 \frac{1}{\delta B_\perp^2} \simeq \frac{\Delta p}{p_1} p_1 \frac{1}{\delta B_\perp^2} \propto B^2 \frac{1}{\delta B_\perp^2} \quad (\text{A12})$$

from eqs.(A8) — (A11).

## REFERENCES

Ayres, T. R. 2000, *Sol. Phys.*, 193, 273

Barnes, A. 1966, *Phys. Fluid*, 9, 1483

Barnes, A. 1968, *ApJ*, 154, 751

Barnes, A. 1969, *ApJ*, 155, 311

Barnes, S. A. 2003, *ApJ*, 586, 464

Belcher, J. W. 1971, *ApJ*, 168, 509

Belcher, J. & MacGregor, K. B. 1976, *ApJ*, 210, 498

Beresnyak, A., Lazarian, A., Cho, J. 2005, *ApJ*, 624, L93

Berghöfer, T. W., Schmitt, J. H. M. M., Danner, R., & Cassinelli, J. P. 1997, *A&A*, 322, 167

Boyd, T. J. M. & Sanderson, J. J. 2003, *The Physics of Plasmas*, Cambridge

Cassinelli, J. P., Brown, J. C., Maheswaran, M., Miller, N. A., & Telfer, D. C. 2002, *ApJ*, 578, 951

Cassinelli, J. P. & Olson, G. L. *ApJ*, 1979, 229, 304

Cassinelli, J. P. & Swank, J. H. *ApJ*, 1983, 271, 681

Charbonneau, P., & MacGregor, K. B. 2001, *ApJ*, 559, 1094

Cho, J. & Lazarian, A. 2002, *Phys. Rev. Lett.*, 88, 245001

Cho, J., Lazarian, A., Vishniac, E. T. 2002, *ApJ*, 564, 291

Cho, J. & Lazarian, A. *MNRAS*, 2003, 345, 325

Cho, J., Lazarian, A., Vishniac, E. T. 2003, *Lec. Not. in Phys.*, 614, 56

Cohen, D. H., Cassinelli, J. P. & MacFarlane, J. J. 1997, *ApJ*, 487, 867

Cranmer, S. R., Field, G. B., & Kohl, J. L. 1999, *ApJ*, 518, 937

Donati, J.-F., Wade, G.A., Babel, J., Henrichs, H.F., de Jong, J.A., & Harries, T.J. 2001, *MNRAS* 326, 1265

Ginzburg, V. L. 1961, *Propagation of Electromagnetic Waves in Plasma*, New York: Gordon & Breach

Hartmann, L. & MacGregor, K. B. 1980, *ApJ*, 242, 260

Henrichs, H.F. 2001, in *Magnetic Fields across the Hertzsprung-Russell Diagram* ASP Conf Ser. Vol 248, 393

Heyvaerts, J. & Priest, E. R. 1983, *A&A*, 117, 220

Hollweg, J. V. 1982, *ApJ*, 254, 806

Jacques, S. A. 1977, *ApJ*, 215, 942

de Jager, C., Nieuwenhuijzen, H., & van der Hucht, K. A. 1988, *A&AS*, 72, 259

Jardine, M., Wood, K., Collier Cameron, A., Donati, J.-F., Mackay, D. H. 2002, *MNRAS*, 336, 1364

Kippenhahn, R. & Weigert, A. 1990, "Stellar Structure and Evolution", *Springer-Verlag*

Lamers, H. J. G. L. M. & Cassinelli, J. P. 1999, 'Introduction to Stellar Wind', Cambridge

Lamers, H. J. G. L. M. & Morton, D. C. *ApJS*, 1976, 32, 715

Lazarian, A. & Vishniac, E. T. 1999, *ApJ*, 517, 700

Leamon, R. J., Mattheaeus, W. H., Smith, C. W., & Wong, H. K. 1998, *ApJ*, 507, L181

Lucy, L. B. 1982, *ApJ*, 255, 286

Lyubarsky, Y. E. 2003, *MNRAS*, 339, 765

MacGregor, K. B. & Cassinelli, J. P. 2003, *ApJ*, 586, 480

Maheswaran, M. & Cassinelli, J. P. 1992, *ApJ*, 386, 695

Michel, F. C. 1969, *ApJ*, 158, 727

Mihalas, D. & Mihalas, B. W. 1984, *Foundation of Radiation Hydrodynamics*, Oxford University Press, section 56

Oughton, S., Mattheaeus, W. H., Dmitruk, P., Milano, L. J., Zank, G. P., & Mullan, D. J. 2001, *ApJ*, 551, 565

Parker, E. N. 1963, 'interplanetary Dynamical Processes', John Wiley and Sons, New York

Parker, E. N. 1966, *ApJ*, 145, 811

Parker, E. N. 1975, *ApJ*, 198, 205

Pizzolato, N., Maggio, A., Micela, G., Sciortino, S., & Ventura, P. 2003, *A&A*, 397, 147

Priest, E. & Forbes, T. 2000, *Magnetic Reconnection*, Cambridge

Seward, F. D., Forman, W. R., Giacconi, T., Griffiths, R. E., Harnden, F. R., Jr., Jones, C., & Pye, J. P. 1979, *ApJ*, 234, L55

Stein, R. F. & Schwartz, R. A. 1972, *ApJ*, 177, 807

Sturrock, P. A. 1999, *ApJ*, 521, 451

Suzuki, T. K. 2002, *ApJ*, 598, 578

Suzuki, T. K. 2004, *MNRAS*, 349, 1227

Suzuki, T. K. & Inutsuka, S. 2005, submitted to *ApJL* (astro-ph/0506639)

Waldron, W. L. & Cassinelli, J. P. 2000, *ApJ*, 548, L48

Weber, E. J. & Davis, L. 1967, *ApJ*, 148, 217

Wood, B. E., Müller, H.-R., Zank, G. P., & Linsky, J. L. 2002, *ApJ*, 574, 412

Wood, B. E., Müller, H.-R., Zank, G. P., Linsky, J. L., & Redfield 2005, *ApJL*, in press (astro-ph/0506401)

Yan, H. & Lazarian, A. 2004, *ApJ*, 614, 757

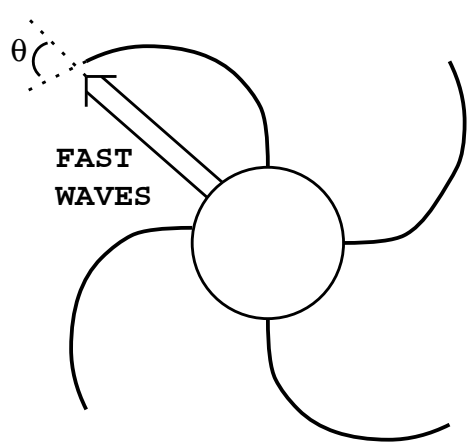


Fig. 1.— Schematic picture of fast MHD waves propagating outward in magneto-rotational wind, illustrating the angle  $\theta$  between the propagation direction and the field at one point in the outer atmosphere.

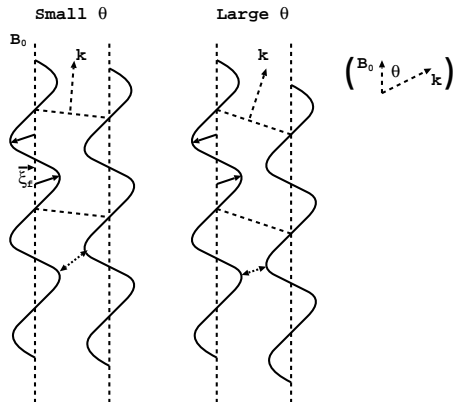


Fig. 2.— Propagation of fast MHD waves for two different angles,  $\theta$ . In a low  $\beta$  plasma, the displacement vector,  $\vec{\xi}_f$ , of the fast mode is almost perpendicular to underlying magnetic field,  $B_0$  (Cho, Lazarian, & Vishniac 2003). This illustrates that the distance between the two oscillating field lines (solid lines) changes more in larger  $\theta$  case than in the lower  $\theta$  case. This is the case even though, as illustrated, the absolute displacements,  $|\vec{\xi}_f|$ , are the same. Particularly, the closest distance between the two field lines (indicated by dotted both-side-arrows) is smaller in the large  $\theta$  case, leading to a more reflective mirror. Hence, a larger number of particles are locked into the surfing on the mirrors. This in turn leads to a higher rate of wave dissipation by particle-field interactions.

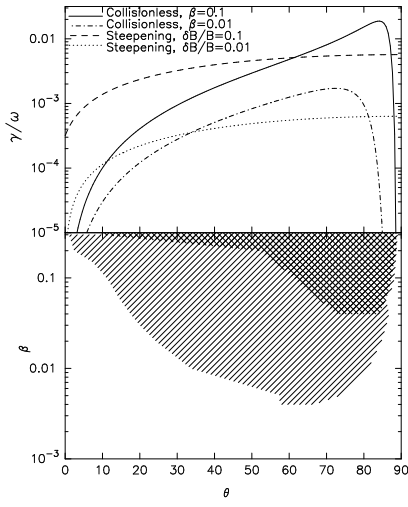


Fig. 3.— *upper*: Comparison of damping rate of the collisionless process with the steepening as a function of  $\theta$ . *lower* : Regions in  $\theta - \beta$  where the collisionless process dominates the steepening for  $dB/B = 0.1$  (cross hatched) and  $dB/B = 0.01$  (single hatched).

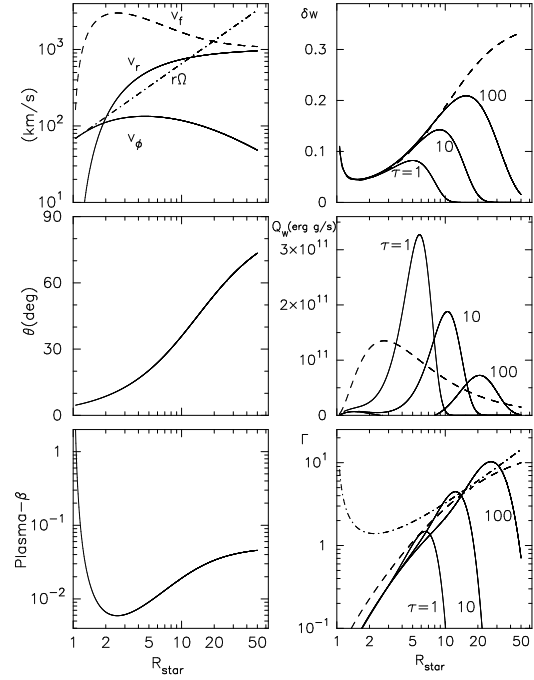


Fig. 4.— Wave dissipation in a solar-type star with  $S_0 = 0.15$ . All the physical quantities are as a function of stellar radius. *Upper left* : velocity structure. *Middle left* :  $\theta$ . *Lower left* : plasma  $\beta$  value. *Upper right* : Normalized amplitude of the fast waves. Solid lines are results with dissipation for three cases of wave period,  $\tau$ . Dashed line is a result without dissipation. *Middle right* : Comparison of heating,  $Q_w$ (erg/g s), for the three  $\tau$ 's (solid) with adiabatic cooling in eq. (21) (dashed). *Lower right* : Comparison of  $\Gamma$ . Solid lines are wave acceleration,  $\Gamma_w$ , dashed line is magneto-rotational acceleration,  $\Gamma_b$ , and dot-dashed line is acceleration by gas pressure,  $\Gamma_g$ .

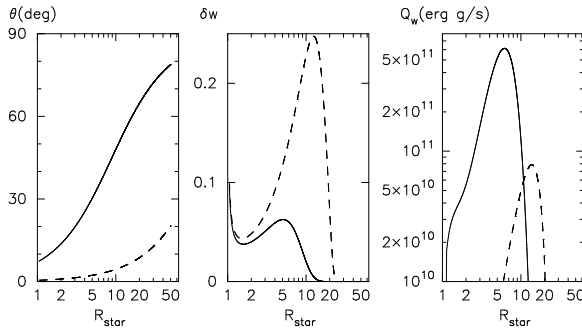


Fig. 5.— Comparison of the propagation angle  $\theta$ , amplitude  $\delta w$ , and heating rate  $Q_w$ (erg/g s) for a fast and slow rotating solar-mass star. The solid lines show results for the fast rotator,  $S_0 = 0.5$ , and the dashed lines refer to the slow rotator,  $S_0 = 0.01$ . Note that the angle and heating rates for the fast rotator are larger, but the wave amplitude (middle panel) for the fast rotator is smaller. This is because it is the radial decrease in the amplitude that leads to the larger heating shown in the right panel.

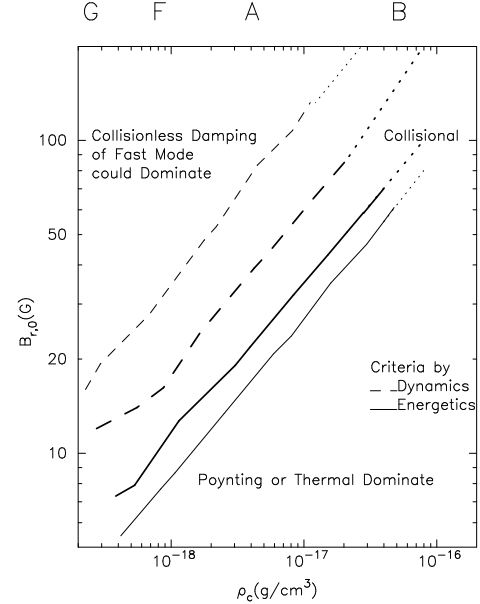


Fig. 6.— Critical magnetic field for collisionless damping of the fast waves as a function of characteristic density,  $\rho_c$  for spin parameter  $S_0 = 0.15$  (thick) &  $0.5$  (thin). We here consider the waves with  $\tau = 1$ (s) and  $\delta w_0 = 0.1$ . Solid lines indicate criteria based on the energetics and dashed lines are those of the dynamics. Upper characters on the top denote corresponding main sequence stars (see text). In upper left region of each line the wave dissipation gives larger contributions to the heating or acceleration than the other processes. In upper right region which is indicated as 'Collisional', the plasma is still collisional even at  $r = 2R_\star$  due to high density so that our process does not work effectively.

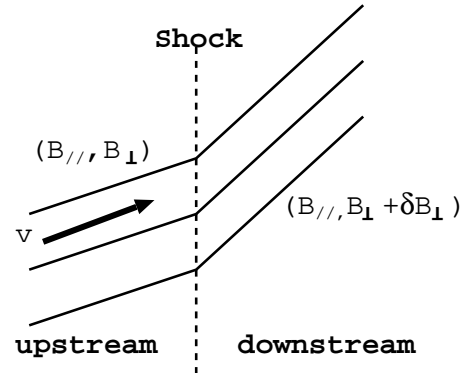


Fig. 7.— Geometry of fast shock.